Available online www.jocpr.com

Journal of Chemical and Pharmaceutical Research, 2014, 6(4):96-100

Research Article

ISSN : 0975-7384
CODEN(USA) : JCPRC5

Dual-band terahertz filters with sharp slope rate of edge based on two-layered composite metamaterial

Zhang-jing Wang*, Shen-hui Guo, Jiang-jiang Li and Fei-ying Wang

School of Electronic Engineering, University of Electronic Science and Technology of China, Chengdu, China
School of Physical Electronics, University of Electronic Science and Technology of China, Chengdu, China

---

ABSTRACT

Terahertz filters with dual-band and sharp slope rate of edge characteristics are reported. We realize the change from single band to dual-band by adding a SRR to the original structure. The mechanism for the dual-band is attributed to introducing a new resonance point. The slope rates of edges for two stop-bands are 297dB/THz, 297 dB/THz, 287 dB/THz, and 354 dB/THz. Tuning bandwidths and center frequencies can be realized by modulating the main parameters of the structure. Besides, the filter is insensitive to the polarization of the THz radiation under g=0 μm.

Keyword: Dual-band, Terahertz filter, Sharp slope rate of edge, Two-layer, Metamaterial.

INTRODUCTION

Recently, terahertz science and technology have received more and more attentions because of its unique properties and potential applications in sensing [1-4], imaging [5-8], and security [9]. Therefore, it is extremely urgent to study the THz devices which can control the transmission power, frequency, phase, or bandwidth of the THz electromagnetic wave such as modulator [10], switch [11], filter [12] etc. Much work has been done for these aims until now.

Considerable progress has been achieved in research of THz devices. Tunable THz switch and triple-resonant terahertz metamaterials have been reported [13-16]. Besides, broadband Filter, tunable THz filter and THz metamaterials with enhanced Q-factor by the effect of spatial arrangement have been published recently [17-19]. In addition, metamaterials with multiple resonances possess considerable potential application in complex and powerful optical devices [20]. So, the study of multiband filter is very meaningful.

EXPERIMENTAL SECTION

1. DESIGN AND SIMULATION RESULTS OF TWO SAMPLES

In this paper, we describe a process that a filter with one stop-band changes to dual stop-bands filter. Fig .1(a) shows a metamaterial based on split-ring-resonator (SRR) structure and its detailed parameters. A square-loop-circle resonator (SL-CR) metamaterial and its structure parameters are shown in Fig .1(b). SRR structure forms a frequency point at f=0.91 THz and SL-CR metamaterial forms a frequency point at f=0.45 THz. By combining SRR and SL-CR metamaterial, we get a square-loop-circle-split-ring-resonator (SL-C-SRR) metamaterial structure and it produces two frequency points f=0.44 THz and f=0.83 THz, as shown in Fig. 1(c). Fig. 1(d) illustrates transmission spectra of three samples with different two-layered structures. Compared the transmission spectra shown in Fig. 1(c) and Fig. 1(d), two-layered structure not only expands bandwidth but also shakes rising edge and trailing edge. All the samples are fabricated on 75 μm thick polyethylene naphthalate (PEN) films. The dielectric constant and the loss tangent of PEN used in our simulations are 2.56 and 0.003, respectively. A 200-nm-thick Al film with conductivity of 3.56×107 S/m is fabricated on PEN. All the simulation results discussed in the following part are offered by the commercial software CST.

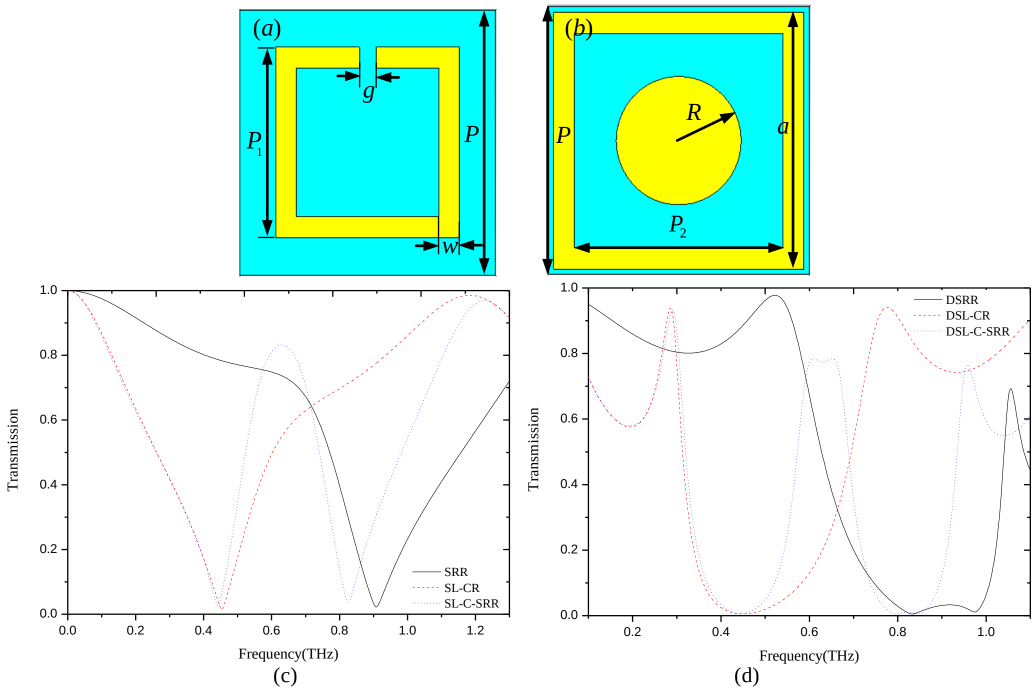

Figure 1. (a) Structural parameters of the SRR unit cell, *P*=125 μm, *P*$_1$=90 μm, *g*=8 μm, *w*=10 μm. (b) the structural parameters of the SLR-C unit cell. *P*=125 μm, *a*=120 μm, *R*=30 μm, *P*$_2$=100 μm. (c) and (d) are transmission spectra of individual sample with different structural for single layer and two layer

2. DESIGN AND SIMULATION RESULTS OF DUAL-LAYER METAMATERIALS

2.1 SAMPLE DESIGN

Fig .2 shows 3-D configuration for two-layered SL-C-SRR metamaterial and its detailed structure parameters. The direction of electric field is perpendicular to the gap and the direction of magnetic field is parallel to the gap as shown in Fig .2 (a). Fig .2 (b) shows a part of the array.

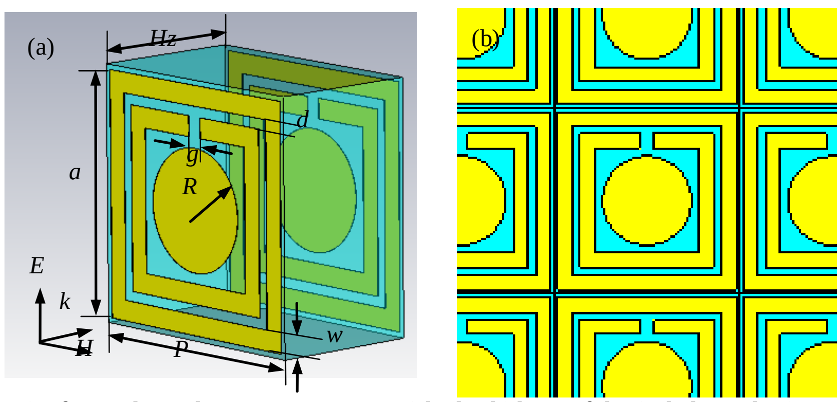

Figure 2. 3-D configuration for two-layered SL-C-SRR metamaterial. The thickness of the single-layer aluminum microstructure is 200 nm. The vectors show the incident THz electromagnetic field orientation. The geometrical parameters of the system are as follows: *a*=120 μm, *P*=125 μm, *R*=30 μm, *w*=10 μm, *g*=8 μm, *d*=5 μm and *Hz*=75 μm

RESULTS AND DISCUSSION

1.1 PARAMETER OPTIMIZATION AND FIELD DISTRIBUTION

Fig .3 shows the transmission spectrum of the SL-C-SRR structure while changing the dimension parameter *P* from 125 μm to 135 μm with space of 5 μm. Two stop-bands both move to higher frequency while increasing *P* and low frequency band range extends broader than high frequency band. The reason for this result is obvious. The increase of *P* results in the increase of inductive. According to formula $f=1/2\pi(LC)^{1/2}$, the increase of *L* results in the decrease of *f*. This is coincident with the Fig .3. The reason for the range of change is elaborated in the following part.

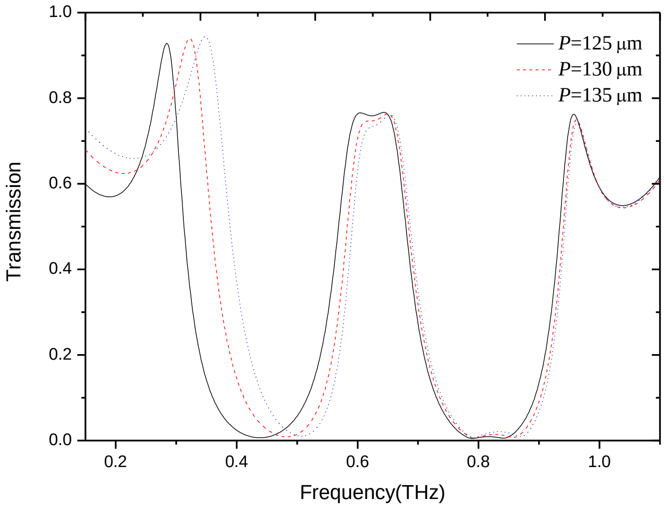

Figure 3. Transmission spectra of the SL-C-SRR structure as adjusting the dimension parameter *P* from 125 μm to 135 μm

In order to deeply understand the characteristics of structure for different periods, we investigated the E-field intensity distributions through numerical simulation in the first layer for the SL-C-SRR under P=125 μm. As illustrated in Fig. 4, at low frequencies 0.15 THz and 0.44 THz, E-field intensity mainly distributes on outer up and down edges. The resonance modes of the two adjacent unit cells are strongly coupled with each other at lower frequencies. For other frequencies, E-field intensity mainly distributes on inner edges as shown in Fig. 4(c)-(e). From these E-field distributions, we can explain why the change range at lower frequencies is lager than high frequencies. Because period P is in outer edges, it mainly influences lower frequencies.

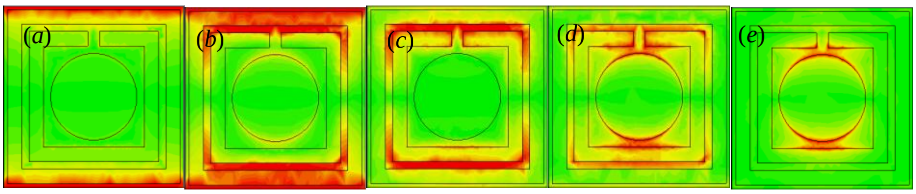

Figure 4. (a)–(e) Simulated magnitudes of electric fields in the top layer of SL-C-SRR at the frequency of 0.15, 0.44, 0.62, 0.81, 1.1 THz when *P*=125 μm, respectively

For such filter design, the main geometry parameters of the structure naturally influence the optical coupling effect. So, we adjust the dimension parameters g and R to investigate the effect of these factors. The curves of transmission spectra with the increasing gap width g are plotted in Fig. 5(a) with P=125 μm. The center of the second stop-band moves to high frequency by changing g from 0 μm to 24 μm. However, the first stop-band hardly changes. The gap g mainly influences high frequencies from the E-field intensity distributions in Fig. 4(c)-(e).

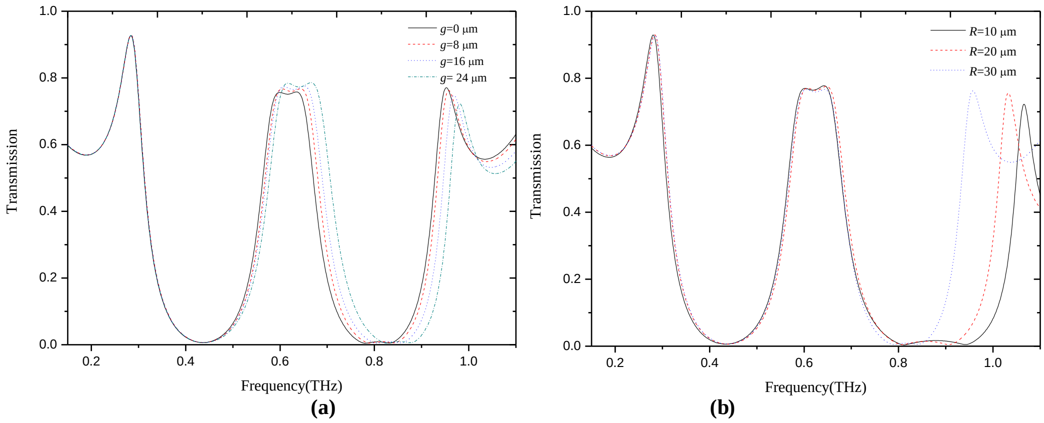

Figure 5. (a) and (b) are transmission spectra of the SL-C-SRR structure when *P*=125 μm as adjusting the dimension parameters *g* and *R*

Fig. 5(b) shows the transmission spectra as increasing the circle radius R. Bandwidths narrowed by changing R from 10 μm to 30 μm. The radius R mainly influences high frequencies from the E-field intensity distributions in Fig.

4(c)-(e). The coupling inductance and capacitance become larger with increasing *R*. So the trailing edge of the second stop-band moves to lower frequency. -30 dB (0.03) bandwidth for the second stop-band is 0.2 THz when *R*= 10 μm.

1.2 OPTIMUM RESULTS

The linear and dB transmission spectra of dual-square-loop-circle-split-ring-resonator (DSL-C-SRR) are shown in Fig. 6(a) and (b). -30 dB (0.03) bandwidths are 0.09 THz and 0.1 THz, respectively. Furthermore, the rising and trailing edges change sharply at a slope rate of 297dB/THz, 297 dB/THz, 287 dB/THz, and 354 dB/THz as shown in Fig. 6(b). This transmission characteristic is better than that reported in Ref [17] and Ref [18].

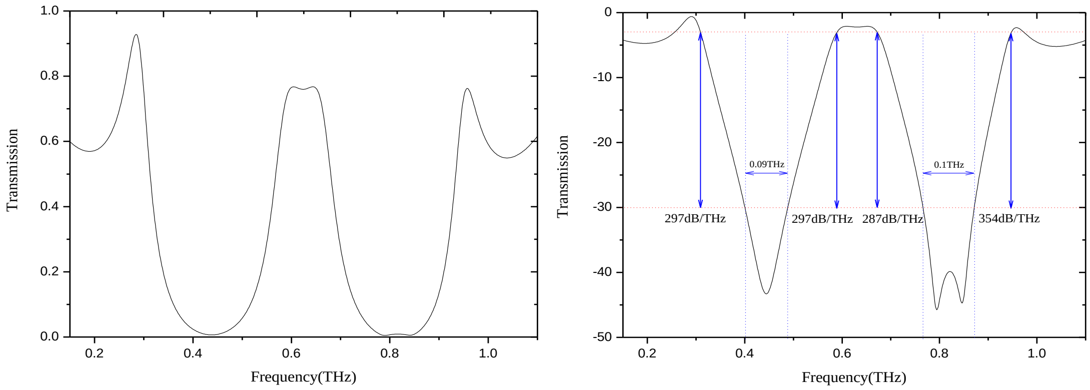

(a) (b)

Figure 6. Linear transmission spectrum of DSL-C-SRR sample for two layers is shown in figure (a) and dB transmission spectrum is shown in figure (b)

2. POLARIZATION STABILITY OF METAMATERIAL

The filter based on SL-C-SRR structure is sensitive to the polarization of the THz radiation. This may limit its application. So, we make inner SRR closed by filling the gap with the same metal of SRR, which means *g*=0 μm. As shown in Fig. 5(a), it also has two stop-bands. Because the new structure dual-square-loop-circle-square-ring-resonator (DSL-C-SRR) in x and y-directions is symmetrical, its transmission spectra is hardly influenced by the polarization of the THz radiation as shown in figure 7(a). Figure 7(b) describes the changes of transmission spectrum with the increasing angle of incidence. Two stop-bands both maintain low transmission values.

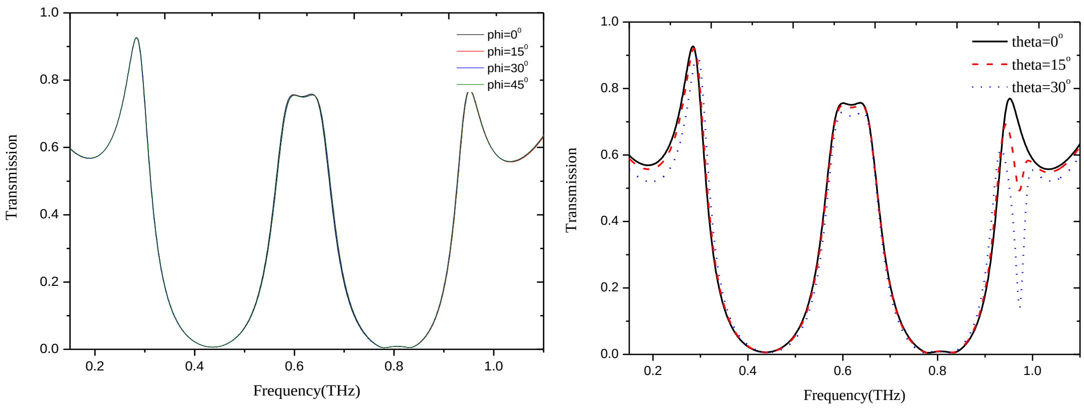

(a) **(b)**

Figure 7. The transmission spectra of SL-C-SRR structure with the SRR closed for different polarization angles phi from 0° to 45° (a) and different angles of incidence from 0° to 30° (b)

CONCLUSION

We present our simulation of dual-band Terahertz Filters. We get two bands with sharp edges by adding two different resonance structures. Through modulating the main parameters of the structure, we gain tuning bandwidths and center frequencies. The period *P* largely influences the first stop-band. However, other parameters of the structure mainly influence the second stop-band. So, two bands are independent with each other.

REFERENCES

[1] D. L. Woolard; E. R. Brown; M. Pepper; M. Kemp, *Processdings of the IEEE*. **2005**, 93(10), 1722-1743.
[2] P. H. Siegel, IEEE Trans. *Microwave Theory Tech*. **2004**, 52(10), 2438-2447.
[3] R. Dickie; R. Cahill; V. Fusco; H. S. Gamble; N. Mitchell; *Terahertz Science and Technology*. **2011**, 1(2), 450-461.
[4] C. E. Groppi; J. H. Kawamura, *Terahertz Science and Technology*., **2011**, 1(1), 85-96.
[5] Li Cheng, Yuichi; Ogawa and Shin'ichiro Hayashi. *Academic J. Cancer Res*., **2013**, 5(12), 887-891
[6] Shraddha Shukla; Anupama Kashyap and Anil Kashyap, *Academic J. Cancer Res*., **2013,** 5(9), 142-145
[7] F. C. De Lucia; MTT-S Int, *Microw. Symp*., **2002**, 3, 1579-1582.
[8] A. Tang; Mau-Chung Frank Chang, *Terahertz Science and Technology*., **2013**, 3(2), 134-140.
[9] N. Palka; M. Szustakowski; M. Kowalski; T.Trzcinski; R. Ryniec; M. Piszczek; W. Ciurapinski; M.Zyczkowski; P. Zagrajek; J. Wrobel, *19th International conference on Microwaves, Radar and Wireless Communications*. **2012**, 265-270.
[10] I. O. Mirza; S. Y Shi; D. W. Prather, *Optics Express*., **2009**, 17(7), 5089-5097.
[11] N.-H. Shen; M. Kafesaki; T. Koschny; L. Zhang; E. N. Economou; C. M. Soukoulis, *Phys. Rev. B*. **2009**, 79, 161102,1-4.
[12] H. T. Chen; J. F. O'Hara; A. K. Azad; A. J. Taylor; R. D. Averitt; D. B.Shrekenhamer; W. J. Padilla, Nat. *Photonics*., **2008**, 2, 295.
[13] N.-H. Shen; M. Massaouti; M.Gokkavas; J.M. Manceau; E. Ozbay, M. Kafesaki, T. Koschny, S. Tzortzakis; C. M. Soukoulis, *Phys. Rev. Lett*., **2011**, 106, 037403, 1-4.
[14] Y.-X. Zhang; S. Qiao; W.-X. Huang; W. Ling; L. Li; S.-g. Liu, *Appl. Phys. Lett*., **2011**, 99, 073111, 1-3.
[15] Abbas Sabah Thajeel; A. Z. Raheem and Mustafa M. Al-Faize, *Academic J. Cancer Res*., **2013**, 5(4), 251-259
[16] Lingfeng LI; Changhui XU; Yunxia Chen and Feng Xiao, *Academic J. Cancer Res*., **2013**, 5(9), 555-562
[17] Z.-Y. Li and Yujie J. Ding, *Journal of Selected Topic in Quantun Electronics*., **2013**, 19(1), 8500705, 1-4.
[18] Y.-S. Lin; Y. Q; F.-S. Ma; Z. Liu; P. Kropelnicki; C. Lee, *Appl. Phys. Lett*., **2013**, 102, 111908, 1-5.
[19] I. Al-Naib; R. Singh; M. Shalaby; T. Ozaki; R. Morandotti, *Journal of Selected Topic in Quantun Electronics*., **2013**, 19(1), 8400807, 1-7.
[20] Y.-J. Chiang; C.-S. Yang; Y.-H. Yang; C.-L. Pan; T.-J. Yen, *Appl. Phys. Lett*., **2011**, 99, 191909.
[21] L.-J. Liang; J.-Q.Yao; X. Yan, Chin. *Phys. Lett*., **2012**, 29, 094209, 1-3.
[22] N. R. Han; Z. C. Chen; C. S. Lim; B. Ng; M. H. Hong, *Optics Express*., **2012**,19(8).